EUROFUSION WPS1-CP(16) 15129

S Marsen et al.

First Results from Protective ECRH Diagnostics for Wendelstein 7-X

Preprint of Paper to be submitted for publication in
Proceedings of 26th IAEA Fusion Energy Conference

This work has been carried out within the framework of the EUROfusion Consortium and has received funding from the Euratom research and training programme 2014-2018 under grant agreement No 633053. The views and opinions expressed herein do not necessarily reflect those of the European Commission.

First Results from Protective ECRH Diagnostics for Wendelstein 7-X

S. Marsen[1], Y. Corre[2], H.P. Laqua[1], V. Moncada[2], D. Moseev[1], H. Niemann[1], M. Preynas[1], T. Stange[1] and W7-X Team[1]

[1]Max-Planck-Institut für Plasmaphysik, Teilintitut Greifswald, Wendelsteinstraße 1, 17491 Greifswald, Germany
[2]CEA-IRFM, F-13108 Saint-Paul-Lez-Durance, France

Corresponding Author: stefan.marsen@ipp.mpg.de

Abstract:

Wendelstein 7-X (W7-X) is a steady state capable optimised stellarator. The main heating system is electron cyclotron resonance heating (ECRH) operating at 140GHz providing up to 9MW microwave power. A set of diagnostics has been developed to protect the machine from non absorbed ECRH power which can easily damage in vessel components. The power is launched into the machine by front steerable quasi-optical launchers in X- or O-mode. While in X-mode the first pass absorption is 99%, it is only 40... 70% in O-mode. The non absorbed power hitting the inner wall is measured by waveguides embedded in the first wall (ECA diagnostic). In order to prevent the inner wall from overheating or arcing, a near-infra red sensitive video diagnostic with a dynamic range of 450...1200°C was integrated in the ECRH launchers. Thermal calculations for the carbon tiles predict a temperature increase above the detection threshold for scenarios of plasma start-up failure or poor absorption on a time scale of 50ms. However, the temperature increase measured by an IR camera in experiments with failed break down, i.e. no ECRH absorption for up to 50ms, was only $\Delta T \approx 70$C.In discharges with $\approx 5\%$ transmission the measured temperature increase was comparable. The stray radiation level inside the machine is measured by so called sniffer probes which were designed to collect all radiation approaching the probing surface independent of incident angle and polarization. Five sniffer probes are installed at different toroidal positions. They were integrated in the ECRH interlock system. During the first operational phase of W7-X this was the only available plasma interlock system. The signal quality proofed to be high enough for a reliable termination in case of poor absorption. After a breakdown phase of 10ms, the sniffer probe signals dropped by more than an order of magnitude. However, especially in the very first days of operation, most discharges died by a radiative collapse due to impurity influx. In this case the heating power was reliably switched off due to the increased level of stray radiation. ECRH bolometers in the launcher ports and an empty diagnostic port were used to estimate the stray radiation level in the ports. In the launcher ports it could be shown than the stray radiation could lead to an overheating of the bellows in long discharges. Possible counter measures are discussed.

1 Introduction

Wendelstein 7-X is an optimised stellarator designed for steady state operation. The main heating system is electron cyclotron resonance heating (ECRH) launching microwaves at 140GHz into the vessel corresponding to the 2nd harmonic of the electron cyclotron frequency at 2.5 T. A quasi optical transmission line is used to bring the power into the machine. The power is launched into the vessel by front steerable quasi-optical launchers from the low field side in X2- or O2-mode [1]. While in X2-mode the first pass absorption is rather high ($\approx 99\%$), it is only 40... 70% in O-mode heating scenarios. The total absorption in O-mode can be increased up to $> 95\%$ using inboard mirrors to allow multipass absorption. Four equatorial launcher ports are used where each of them has three individual beam lines. Each beam line corresponds to one gyrotron which was designed for up to 1MW cw power. During the first operational phase of W7-X (OP 1.1) 6 gyrotrons providing up to 4.3MW microwave power were available as the sole heating system. The gyrotrons were operated at reduced power of 600 . . . 800kW to increase the reliability of the ECRH system. The total injected energy was limited to 4MJ in order to protect in vessel components, especially the five poloidal limiters, from overheating. For the next operational phases 4 additional gyrotrons will be brought into operation and the control system will be optimised aiming to provide 9MW port through heating power. This paper reports on the experience regarding the safe operation of the ECRH system gained from OP 1.1.

Non absorbed ECRH power can easily damage in vessel components by arcing or overheating. Overheating is an issue especially in long discharges which are one of the major goals of W7-X. A lot of effort has been spent on the protection of components from thermal loads during the designs phase of W7-X. However, this passive protection is only efficient up to a certain level. Therefore, a set of diagnostics has been developed to protect the machine from non absorbed ECRH power. Two types of possibly dangerous microwave radiation have to be considered. Direct impact of the microwave beams after the first pass or a few reflections is an issue close to the launching position and can lead to arcing or overheating on short time scales (< 1s). After multiple reflections a more or less isotropic stray radiation background occurs which has much lower power densities than directed beams. Stray radiation is present anywhere in the vessel and can cause damage in longer discharges.

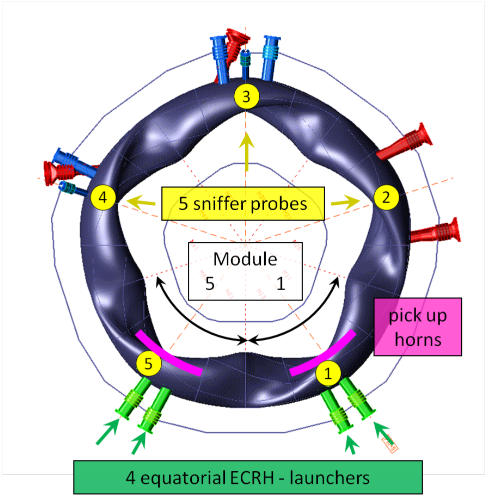

FIG. 1: Top view of the W7-X vacuum vessel. The position of the ECRH launchers is shown in green together with the sniffer probes (yellow) and the ECA diagnostic.

For the observation of direct beam impact two dedicated ECRH protective diagnostics were installed. Pick up horns embedded in the first wall opposite the launchers are used to couple out and detect a fraction of the non absorbed power after the first path. This so

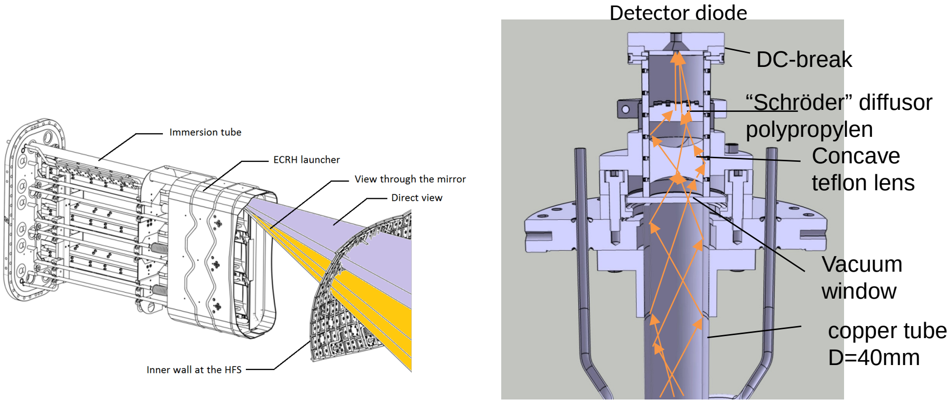

(a) NIR video diagnostic (b) Sniffer probe design

FIG. 2: (a) Drawing of the ECRH launcher with the immersion tube for the NIR video diagnostic. The view is split in two half cones by a mirror in order to observe the entire shine through area. (b) Design of the back end of the sniffer probes. The concave lens together with the Schröder diffuser provide a broad antenna pattern.

called ECA diagnostic is relatively calibrated on a shot to shot base. ECRH is generally used for plasma start up in W7-X. Therefore there is always a short period (5 . . . 20ms) with no absorption before breakdown. The power level measured during this period marks 100% transmission. During OP 1.1 the calibration of the ECA diagnostic with full power turned out to be difficult due to arcing at the antenna opening. Therefore it was mostly used with low power diagnostic beams.

In order to observe arcing and overheating of the first wall tiles a near infra red video diagnostic was installed in immersion tubes in the ECRH launchers as shown in fig. 2 (a) [2]. It uses visual to NIR analog cameras along with a 920nm long pass filter. The field of view is split in two half cones by a mirror in order to be able to observe the entire shine through area opposite the launchers. The upper part of the wall is in the direct view of the camera (purple cone in fig. 2 (a)). In order to observe the lower part of the wall, a stainless steel mirror was installed in front of the optics (yellow cone). The dynamic range of the video diagnostic is between 450 and 1200°C which is well within the specified safe operating range of the inner wall tiles. Although predicted by thermal calculations no heating of the first wall tiles above the detection threshold by ECRH shine through was observed during OP 1.1. The NIR video diagnostic proved to be useful for arc detection. Arcs occurred at the tile edges and screw holes during start up or after a radiation collapse, i.e. in phases with no absorption. They could usually be mitigated by small corrections of the launching angle. The shine through area in module 5 is also observed by an IR camera which is sensitive up to ≈ 350°C. The results presented in section 3 rely on data from this camera.

Stray radiation is observed by 5 so called sniffer probes which are distributed around the torus as shown in fig. 1. They were designed to measure radiation from any direction, i.e. to have a broad antenna pattern. This is achieved by installing a concave lens and

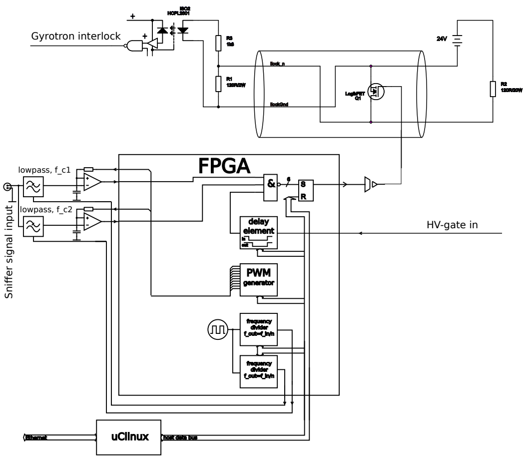

(a) Sniffer probe interlock

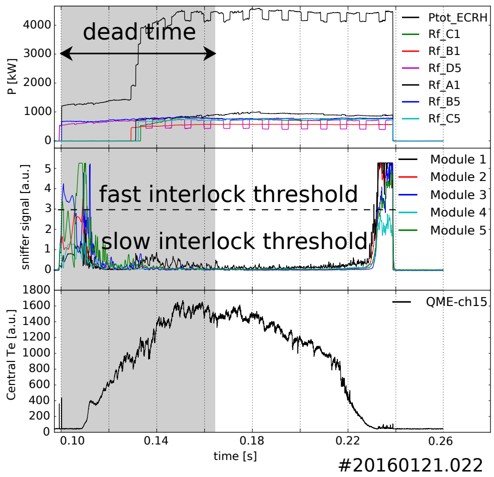

(b) Radiation collapse

FIG. 3: (a) Principle of the ECRH interlock where the sniffer probe signals were intergrated. (b) Time traces of a pulse terminated by the sniffer interlock after a radiation collapse. The stray radiation level increases rapidly when T_e falls below a certain threshold.

a Schröder diffuser at the end of an oversised wave guide which acts as actual antenna. The sniffer probes were absolutely calibrated before OP1.1 [3] to allow measuring the distribution of stray radiation around the torus. Another concern regarding stray radiation is the level inside ports. These are equipped with stainless steel bellows which connect the plasma vessel with the outer cryostat vessel. These must not heat up by more than $\Delta T = 80°$C. Stainless steel absorbs $\approx 1\%$ of incoming microwave power. From the material properties one can calculate the maximum allowed level of stray radiation P^{max}_{stray} in the vicinity of an uncooled bellow. For a discharge duration of 1800s the maximum ΔT would be reached at $P^{max}_{stray} = 8.6\text{kWm}^{-2}$. The temperature of the bellows is monitored by thermocouples in one diagnostic port in module 5 which was empty during OP1.1. Also the bellows of two ECRH launchers are equipped with thermocouples. P_{stray} in the launcher ports is expected to be higher than in the torus or in diagnostic ports because a fraction of the beam can be peeled off at the mirrors in the launcher. Since no significant temperature increase of the bellows was expected during the pulsed operation in OP1.1 special microwave bolometers were designed and installed close to the thermocouples. These are small cylinders of copper coated with a microwave absorber absorbing $> 80\%$ of the microwave power at 140GHz. From the ΔT during a pulse measured by thermocouples inside the bolometer and the pulse duration t_{pulse} one can calculate the average P_{Stray} in the vicinity of the bellows during a pulse, $< P_{stray} >= 5.7\text{kWm}^{-2}\text{sK}^{-1}\Delta T t^{-1}_{pulse}$.

2 Stray radiation interlock

The amount of unabsorbed microwave energy in the torus was for safety reasons limited to 200kJ per pulse during OP1.1. So, with full power of 4MW it was only allowed to operate the ECRH for 50ms with no or poor absorption. The sniffer probe signals were integrated in the existing fast interlock system of the ECRH control system [4]. This was the only available plasma interlock system during OP1.1. The principle of the fast interlock system is shown in fig. 3 (a). The system is mostly used for arc detectors along the ECRH transmission line. Fast comparators with a programmable threshold (pulse width modulation output of FPGA) act as input. An input signal below the programmed threshold is detected by an FPGA which then sets an output signal that shortens the so called interlock bus. If no signal is detected at the terminating resistor of the bus the gyrotron is switched off within a few μs. The electronics of the interlock system was upgraded for the integration of the sniffer signal to fulfil two special requirements. Firstly, the sniffer interlock must not be active immediately after switching on the first gyrotron. A certain (ideally programmable) delay time is necessary to allow for an absorbing plasma to build up. This delay time was typically set to 65ms during OP1.1. Secondly, the sniffer signals may be quite noisy and one wants to allow short periods with higher stray radiation levels. Therefore, programmable low pass filters were installed at the signal inputs. Each of the 5 sniffer signals was connected to two inputs with different integration times and thresholds. A fast (typically $\tau = 10$ms) channels with a relatively high threshold and a slow ($\tau = 50$ms) with a lower threshold. The fast channel is supposed to switch off in case of a sudden loss of absorption, e.g. a radiation collapse. The slow channel would prevent a gradual loss of absorption, e.g. when approaching the cut-off density. Fig. 3 (b) shows a typical example where an experiment program was terminated by the sniffer interlock after a radiation collapse. The sniffer signals show a strong peak at the very beginning which drops by more than an order of magnitude within the first 20ms. The central electron temperature reached a maximum at $\approx$ 50ms and started decaying from there on. This loss of temperature was due to impurity influxes from the wall. At the end of the pulse T_e was too low for X2-mode absorption as seen by the quick rise of the sniffer probe signals. After the integration time of 10ms the fast interlock channel switched off the gyrotrons. Due to poor machine conditioning many pulses were terminated by the sniffer interlock after a radiation collapse. The interlock system proved to work very reliably. We analysed more than 500 pulses, 150 of which had a too low T_e at the end indicating a radiation collapse. The sniffer interlock reacted in every case where it was supposed to, i.e. where the signal was above the threshold. There were two pulses, where the interlock was triggered later than the programmed integration time. Here the sniffer probe showed a level above the fast interlock threshold for $\approx$ 70ms. The reason for this is unknown.

3 Heating of the first wall

The first wall of W7-X is covered with graphite tiles which are mounted on a CuCrZr support structure. The latter will be actively cooled later during steady state operation. During OP1.1 only part of the graphite tiles were installed. The ECRH shine through area was fully covered. The temperature limit of the graphite tile was set at 1200°C which would be in the range of the NIR video diagnostic. When exposed to microwaves at 140GHz graphite absorbs up to 10% of the power. Thermal calculations of the expected temperature rise were done before OP1.1 assuming different power levels. Here we assumed a 600kW beam with a width of $w = 30$mm at a power density of Q_{max}/e^2 ($Q_{max} = 2/\pi P/w^2 = 424\text{MWm}^{-2}$). Thus, the heat flux absorbed by the tiles is $Q_n = 42\text{MWm}^{-2}$ with 100% transmission of the plasma.

Fig. 4 shows in blue the surface temperature of a tile during a failed break down measured by the IR camera. The ECRH was on for 50ms before being switched off by the sniffer interlock in this case. The measured temperature increase was only $\approx 70°$C.

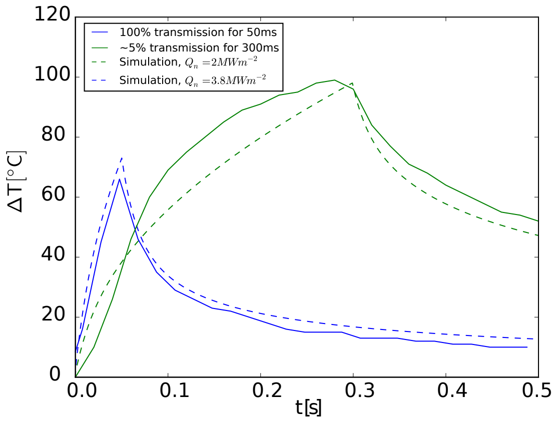

FIG. 4: Experimentally observed increase of the surface temperature for different transmission of the plasma compared to simulation results.

Surprisingly, with only $\approx 5\%$ transmission the measured temperature increase was only slightly slower (green curve in fig. 4). In this case the beam hit the tile under observation after passing the plasma three times in O-mode. The single pass absorption was here $\approx 60 \ldots 65\%$. In the simulations a heat flux of $Q_n = 2\text{MWm}^{-2}$ for the O-mode shot and $Q_n = 3.8\text{MWm}^{-2}$ for the failed breakdown were assumed to reproduce the experimentally observed temperature increase. The temporal evolution of ΔT deviates from the experimental data for the O-mode case. This is reasonable because the plasma density was increasing during the O-mode heating phase leading to an increase of absorption with time. The heat flux was therefore continuously decreasing over time leading to a steeper ΔT in the beginning. In the simulations Q_n was assumed to be constant. The assumed $Q_n = 2\text{MWm}^{-2}$ agrees well with the assumption of 5% transmission.

However, with 100% transmission the heat flux assumed in the simulations is one order of magnitude lower than expected. Although this is beneficial in terms of machine safety because no critical temperature increase of the tiles was observed during OP1.1, the reason for such contradictory results is currently not understood and under discussion. Possible sources of error are the beam width with an uncertainty of $\pm 20\%$ and the absorption coefficient of the graphite tiles where 10% is a worst case assumption. Values of $5 \ldots 10\%$ are possible here. The lowest possible peak heat flux within these errors is $Q_n = 15\text{MWm}^{-2}$ which is still a factor of ≈ 4 off the assumed heat flux in fig. 4.

4 Stray radiation in ports

The ECRH bolometers in the ports proved to be sensitive enough for stray radiation measurements even for short pulses with $t_{pulse} < 1$s. During an experiment on electron cyclotron current drive we performed a shot by shot scan of the toroidal launching angle of some gyrotrons. $\Phi = 0°$ refers to a launching angle perpendicular to the magnetic field lines on axis. In the launcher ports equipped with bolometers there was only one gyrotron each in operation. Fig. 5 shows the temperature increase of the bolometers during the scan. In port AEA10 the gyrotron C1 was active. In port AEA51 it was gyrotron D5. Each peak in the ECRH power corresponds to one pulse of 1s. The gyrotrons were operated at 600kW. P_{stray} as derived from the temperature increase in each pulse varied between $1.7 \ldots 8.5$ kWm^{-2}. The highest levels were observed for $\Phi < 0°$. For the worst case the maximum allowed level would be clearly exceeded for more power injected in one launcher. The lowest levels occurred at $\Phi \geq 0$. The results shown here for perpendicular launching angles agree well with those from other pulse durations and power levels in the launchers. Extrapolating $P_{stray} = 1.7$kWm^{-2} at 600kW to the maximum power of 3MW in each launcher port (3 gyrotrons at the full power of 1MW each) leads to $P_{stray} = 8.5$kWm^{-2} which is very close to the maximum allowed level. In the diagnostic port AEM51 no significant level of stray radiation was observed for any X2-mode pulse. Here the plasma absorbs the power launched into the machine almost completely leading to very low levels of stray radiation. In O2-mode levels of $P_{stray} \approx 5$kWm^{-2} were found in the AEM51 port. This agrees well with the maximum $P_{stray} \approx 7$kWm^{-2} seen by the sniffer probe in module 2. The O-mode heating power in this case was 2.5MW. Thus, with the full available 10MW heating power one would expect $P_{stray} \approx 20$kWm^{-2}. This is compatible with the design criteria for in vessel components of W7-X. It was previously decided that all in-vessel components have to withstand a power flux density of ECRH stray radiation of 50kWm^{-2} [5]. The bellows in diagnostic port will be hardened against stray radiation in future when steady state operation is envisaged. Otherwise they would clearly overheat in this scenario. However the result is not necessarily representative for later O2-mode operation in W7-X. The density in this case was below the X2 cut off density of $1.2 \cdot 10^{20}$m^{-3}. The major goal of O2-mode heating is the ability to operate at higher densities where X-mode waves can't penetrate the plasma anymore. This will affect the distribution of stray radiation in the torus which depends on the plasma as an absorber for stray radiation. At high densities the plasma won't absorb the X-mode content of the stray radiation which may lead to a higher level.

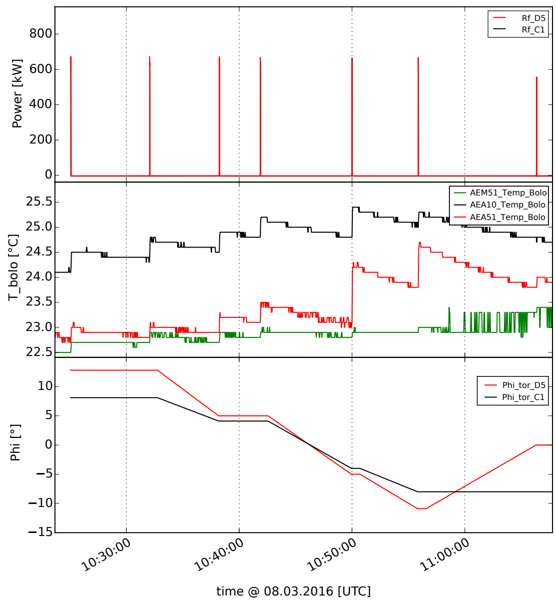

FIG. 5: (a) Temperature of the ECRH bolometers in the launcher and diagnostic port during a shot by shot scan of the toroidal launching angle.

5 Conclusions

The protective ECRH diagnostics of W7-X contributed significantly to the success of the first operational phase of W7-X. ECRH was the sole heating during OP1.1. Especially the proven reliability of the sniffer interlock allowed a quick extension of the pulse length throughout the experimental campaign from some 10ms in the very first days up to 6s towards the end. The quality of the sniffer probe signal was good enough for an automatic detection of a loss of absorption and to trigger an interlock for the ECRH control system. The ECRH bolometers installed in the launcher ports showed stray radiation levels which would overheat the bellows inside the port in steady state operation. Several counter measures are under discussion at the moment. One could install actively cooled microwave absorbing material inside the port. If their surface is large enough they would significantly reduce the stray radiation level in the port. Another solution would be to cover the bellows with copper which absorbs significantly less microwaves than stainless steel and would therefore heat up less than the bellows.

The heating of the first wall by ECRH shine through was expected to be much higher from thermal calculations than actually observed in the experiments. The NIR video diagnostic integrated in the launchers never observed a temperature increase above the detection threshold of 450°C.

The NIR video diagnostic was useful for arc detection during OP1.1. Arcs occurred regularly during start up at the gaps between tiles or at the screw holes. These could be observed by the cameras and in some cases mitigated by small corrections of the launching angle.

References

References

[1] V Erckmann et al. *Fusion science and technology*, 52(2):291–312, 2007.

[2] M. Preynas et al. *Review of Scientific Instruments*, 86(11), 2015.

[3] D. Moseev et al. *Review of Scientific Instruments*, 87(8), 2016.

[4] Georg Michel. *Fusion Engineering and Design*, 74(14):611 – 615, 2005.

[5] D. Hathiramani et al. *Fusion Engineering and Design*, 88(68):1232 – 1235, 2013.

This work has been carried out within the framework of the EUROfusion Consortium and has received funding from the Euratom research and training programme 2014-2018 under grant agreement No 633053. The views and opinions expressed herein do not necessarily reflect those of the European Commission.